iris aperture (source of the short range wakes) with respect to the axis of the cell and damping waveguides (measuring the wakes) must be at least better than 3.5 micrometers.

In summary, micrometer tolerance level is required in cell disk fabrication and several micrometers in the structure assembly in order to satisfy stringent beam dynamics requirements without additional tuning.

2.6.7 References

1. A. Grudiev, H. H. Braun, D. Schulte, W. Wuensch, "Optimum Frequency and Gradient for the Clic Main Linac Accelerating Structure", LINAC08, Victoria, BC, Canada, (2008).
2. A. Grudiev, W. Wuensch, "Design of X-band accelerating structure for the CLIC main linac", LINAC08, Victoria BC, Canada, (2008).
3. ANSYS HFSS, http://www.Ansoft.com
4. M. Luong, I. Wilson, W. Wuensch, "RF Loads for the CLIC Multibunch Structure", PAC'99, New York, 1999.
5. A. Grudiev, S. Calatroni, and W. Wuensch, "New local field quantity describing the high gradient limit of accelerating structures", Phys. Rev. ST Accel. Beams 12, 102001 (2009).
6. W. Bruns, http://www.gdfidl.de
7. F. Peauger, et.al, "Wakefield monitor development for CLIC accelerating structure", LINAC10, Tsukuba, Japan, (2010), CERN-ATS-2010-220.
8. R. Zennaro, "Study of the machining and assembly tolerances for the CLIC accelerating structure", EUROTeV-Report-2008-081, (2008).

2.7 CLIC Power Extraction and Transfer Structure

Igor Syratchev, CERN, CH 1211 Geneva 23, Switzerland
Mail to: Igor.Syratchev@cern.ch

The generation of short (250 ns) high peak power (135 MW) RF pulses by decelerating a high current (100 A) bunched (12 GHz) drive beam is one of the key components in the CLIC two beam acceleration scheme. The CLIC PETS is a low impedance, high group velocity iris loaded 0.213 m long structure with a relatively large ($2\ a/\lambda = 0.92$) beam aperture. Each PETS is comprised of eight octants separated by damping slots. Each slot is equipped with damping loads in order to provide the strong damping of the transverse higher order modes [1]. In operation, the high peak power RF pulses (135 MW × 240 ns) are generated in the PETS via interaction with a high current (100 A) bunched (12 GHz) drive beam. These pulses are extracted at the downstream end of the PETS using a special high power coupler and are distributed to the two CLIC accelerating structures using an RF waveguide network. The snapshot of such a process simulated with computer code T3P [2] is shown in Fig. 1.

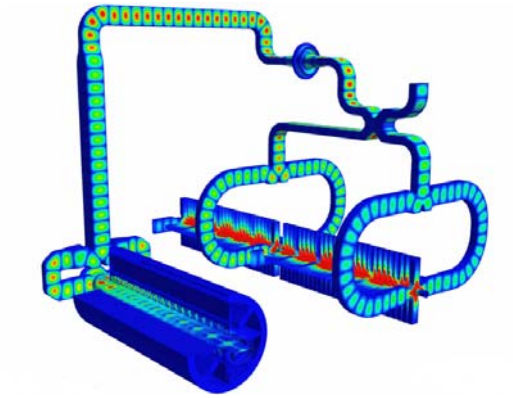

Figure 1: Electric filed plot in the CLIC two-beam accelerator unit. Here the PETS (shown left) is driven by the steady state drive beam current (courtesy SLAC).

During the period of 2008-2012, a thorough high RF power testing program was conducted at CERN in order to demonstrate experimentally the feasibility of all the issues associated with high RF power generation using the drive beam. In parallel, complimentary tests using X-band high power klystrons as a RF power source were done at ASTA (SLAC). Operated at a repetition rate of 60 Hz, such experiments provided high enough statistics to quantify the RF breakdown trip rate. To do these tests, an 11.424 GHz scaled version of the 12 GHz PETS was designed and fabricated, see Fig. 2. The feasibility of the PETS operation at a peak RF power level ~7% higher and with RF pulses ~10% longer compared to CLIC requirements was successfully demonstrated in these experiments [3]. The tests at a fixed power level (see Fig. 3) were ended when the measured breakdown trip rate was close enough to the CLIC specification of 1.0E-7/pulse/m. In the ASTA test, it occurred after 80 hours of operation without breakdown (BDR <2.4E-7/pulse/m).

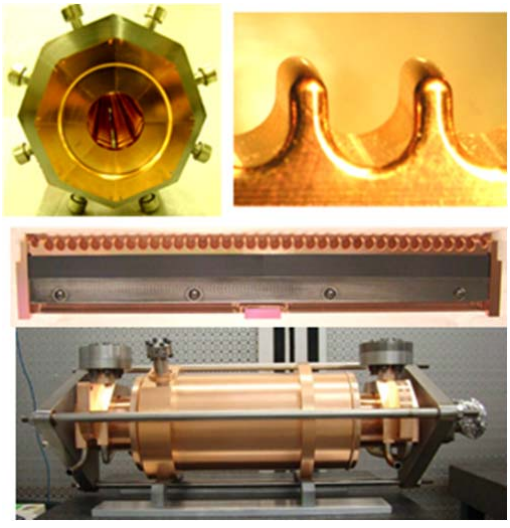

Figure 2: The front view of the assembled PETS body (top left), zoom of the PETS single bar period (top right), the single bar equipped with damping loads (centre) and fully assembled structure (bottom).

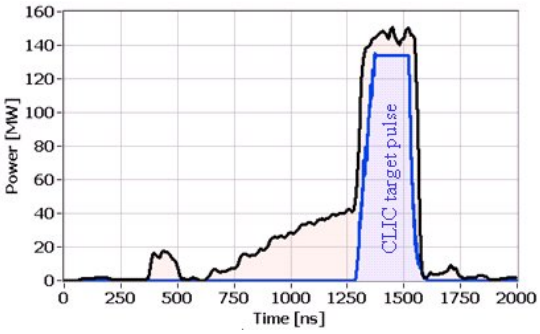

Figure 3: Typical RF pulse shape in ASTA. Here, for convenience, we also have plotted the shape of the CLIC target pulse.

2.7.1 PETS Testing Program in CTF3

2.7.1.1 *PETS Operation at Two Beam Test Stand*

The generation in the PETS of 12 GHz RF power from the drive beam was demonstrated in the CLIC experimental area (CLEX), which is a part of the CLIC Test Facility (CTF3) [4]. The CLEX is equipped with a number of experiments. One of them is the Two Beam Test Stand (TBTS). The TBTS is a unique and versatile facility where the two-beam acceleration experiments are conducted. It comprises two beam lines equipped with various types of beam diagnostics. One line is for the drive beam, which is generated in the CTF3 complex and then delivered to the TBTS via a beam transfer line, the other is dedicated to the probe beam, which is prepared in the CALIFES accelerator complex. As it is shown in Fig. 4, CTF3 will allow for different scenarios of the drive beam generation in terms of the beam current and pulse length.

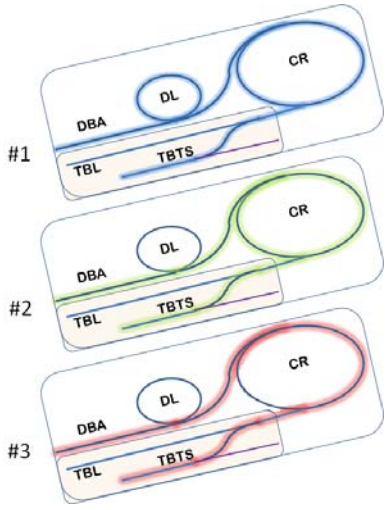

Figure 4: The drive beam generation modes in CTF3: 1– with full recombination (×8), 2 – with partial recombination (×4), and 3 – without recombination.

Because the drive beam current available in CTF3, even with full recombination, will be about four times lower than the CLIC design, the TBTS PETS design was

modified to be able to generate the nominal CLIC RF power. To recover the lack of current, the active PETS length was significantly increased from original 0.213 m to 1m. The fully assembled, 1 meter TBTS PETS equipped with water cooling channels and power couplers on its girder and ready for the installation into the vacuum tank is shown in Fig. 5. The TBTS PETS power production capability for the different CTF3 modes of operation (assuming the single bunch form factor =1) is summarized in a Table 1. Mode 1 of the PETS operation provides power levels well above CLIC nominal values; unfortunately, the pulse length of 140 ns is rather short compared to the CLIC nominal pulse of 240 ns. To improve this, it was decided to implement a different configuration – PETS with external re-circulation [5]. In this case, the PETS operates in an amplification mode, similar to that in the classical resonant rings. The only difference is that now we have a beam as an internal source of RF power.

Table 1: The TBTS PETS power production modes

Operation mode	#1	#2	#3
Current, A	<30	14	4
Pulse length, ns	140	<280	<1200
Bunch Frequency, GHz	12	12	3
PETS power (12 GHz), MW	<280	61	5

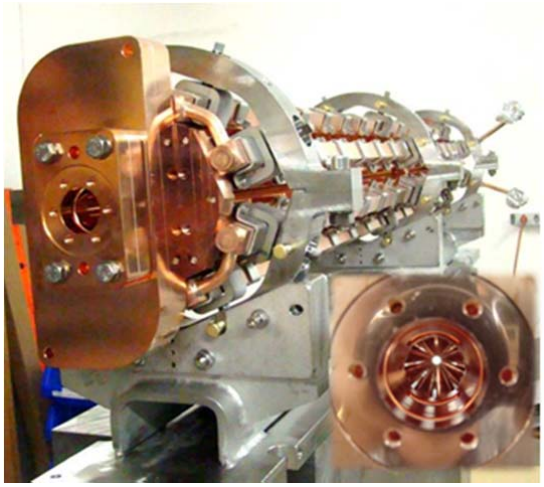

Figure 5: The TBTS PETS general view.

The implementation of re-circulation required development of several special RF components. High RF power variable splitter and variable (2π) RF phase shifter were ordered and received from industry (GYCOM, Russia) [6]. In 2008, a PETS tank equipped with all the RF components was installed into the drive beam line in the TBTS experimental area, as is shown in Fig. 6. With re-circulation, the power gain of the system in a steady can be written as:

$$P_G = \frac{1}{1 - 2g\cos(\phi) + g^2} \qquad (1),$$
$$g = \sqrt{S\eta_{loop}}$$

where S is fractional power delivered back to the PETS input, ϕ is RF phase advance in the loop and η_{loop} is total round trip efficiency. Following (1), in a phased loop (ϕ=0) with 50% re-circulation (S=0.5) and 75% measured ohmic efficiency (η_{loop}=0.75), the steady state power gain is about 6.5. Thus, driven with only 8.6 A drive beam current, the PETS generates the required CLIC RF peak power. At the same time, the RF power extracted from the re-circulating loop (50%) and received by the single accelerating structure would also be as high as required. Providing enough margin in drive beam current and pulse length, the PETS operation mode 2, together with ~50% re-circulation was chosen as a working point for the PETS power production and two-beam acceleration program. In this configuration, the TBTS PETS was operated until September 2011. After start up and initial conditioning, it was reliably generating RF peak power well in excess of the CLIC nominal value. In Fig. 7 the example of a typical pulse generated at the PETS output is shown. One can see clearly the expected stair-case nature of the RF power build-up, where the duration of each step corresponds to the round-trip delay in the re-cycling loop.

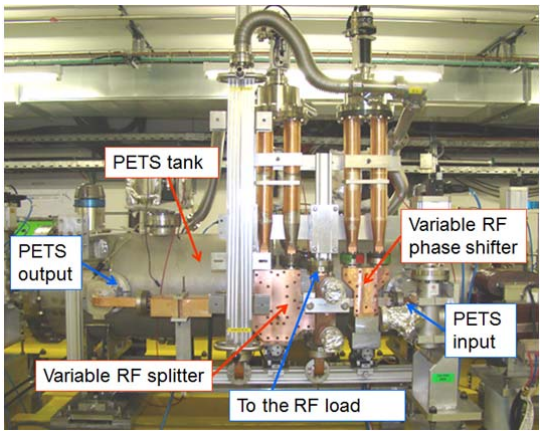

Figure 6: The PETS tank installed in the TBTS test area.

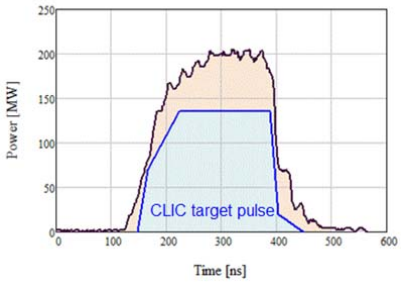

Figure 7: Typical RF pulse shape measured at the PETS output. Here, for convenience, we also plotted the shape of the CLIC target pulse.

We have developed a number of computer models of varying complexity which accurately reconstruct and predict the processes in the system with re-circulation [7-9].

In order to illustrate this, in Fig. 8 and Fig. 9, the simulated results are compared to measurements. In this example, we used a rather simple model [9] based on the known settings of re-circulation (ϕ and g) and measured profile of the drive beam current. One can see good agreement between the simulations and experiments.

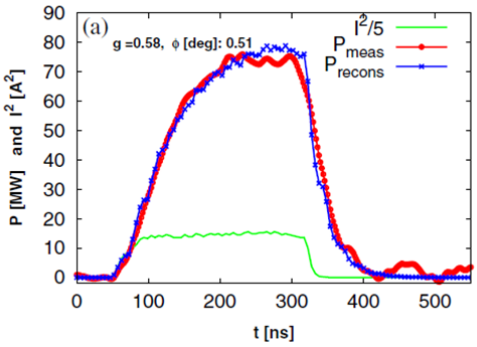

Figure 8: Measured RF pulse (red line) and reconstructed signal (blue line) are shown together with the current pulse used as an input for reconstruction (green line).

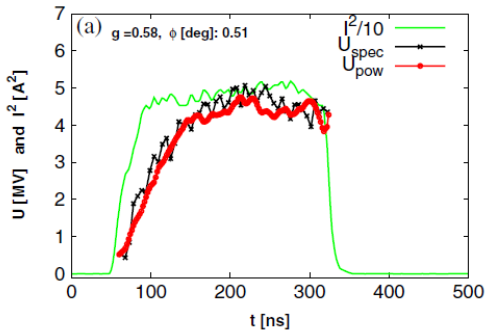

Figure 9: Measured with the spectrometer the drive beam deceleration (black line) and the one calculated from power measurements (red line) are shown together with the pulse current (green line). It shows the same pulse as in Fig. 8.

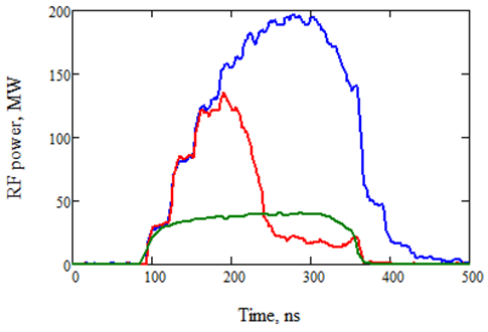

Figure 10: The normal RF pulse (blue line) followed by the RF pulse with breakdown (red line). Here the expected direct (without re-circulation) RF power production (green line) is shown for the reference.

Here we cannot give a firm conclusion about the breakdown trip rate in our experiments in the TBTS, because of insufficient statistics (CTF3 operates at 1 Hz

repetition rate) and some difficulties with providing stable drive beam generation during long enough periods. Nevertheless, an important observation concerning the pulse shape modifications due to the RF breakdown was made: power production is normally quenched just after the RF breakdown happens. This may be explained by the fact that the RF breakdown products modify the gain and phase advance in the loop. In most of the cases (>90%), the PETS continued to generate RF power at a much lower level, which is close to the direct power production level, see Fig. 10. This indicates that most probably, the breakdown happened in the re-cycling waveguide loop and not the PETS itself. Relying on this "self-protecting" effect, a quite aggressive operational procedure was implemented, where the control system followed up the integrated level of residual gas pressure in the PETS tank, rather than reacting on each individual breakdown event.

2.7.1.2 *Demonstration of the PETS ON/OFF Operation*

One of the feasibility issues of the CLIC two-beam scheme, is the possibility of rapidly switching off the RF power production in an individual PETS in case of breakdowns, which can occur either in the PETS or one of the main beam accelerating structures. The proposed solution is to use a variable external reflector connected to the PETS. When activated, this scheme allows us to continuously manipulate the RF power transfer to the accelerating structure and to reduce the RF power production in the PETS itself by a factor of 4 [10].

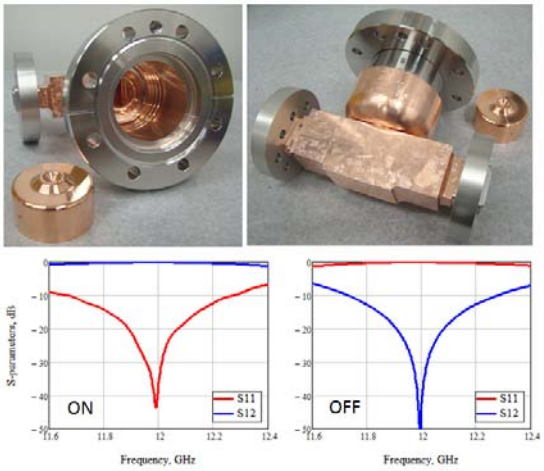

Figure 11: The general view of the variable reflector body and movable piston (up). S-parameters measured at two extreme positions of the piston.

An external high power variable RF reflector is the key component of the system [11]. Providing the whole range of reflections from 0 to 1, it can fully or partially terminate the RF power transfer from the PETS to the accelerating structure. In general, the reflected RF power will be returned back to the PETS. In order to mitigate this effect, a fixed RF reflector is placed at the upstream end of the PETS, in order to establish re-circulation of the RF power inside the PETS. If, at the operating frequency, the electric length of such an RF circuit is tuned to $L=\lambda_0(n+1/4)$, then a destructive interference with the RF power generated by the drive beam is achieved. A prototype of the new high RF power variable reflector was fabricated and low RF power measurements were in good agreement with HFSS [13] simulations, see Fig. 11. We

also built a separate variable RF short circuit to enable the tuning of RF phase advance in the system. In 2011, these new components replaced the external re-circulation circuit on the TBTS PETS tank as shown in Fig. 12.

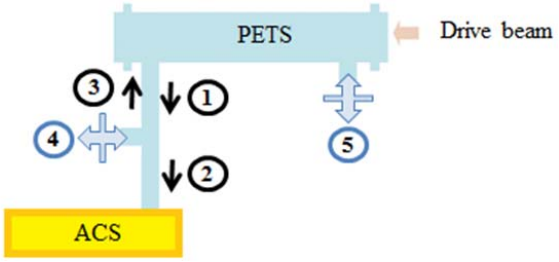

Figure 12: Layout of the PETS ON/OF setup in TBTS. The black arrows show RF power flows in the system: 1) RF power extracted from the PETS; 2) RF power transmitted to the accelerating structure; 3) RF power reflected back into the PETS. The new components are: 4) variable RF reflector; 5) variable RF short circuit.

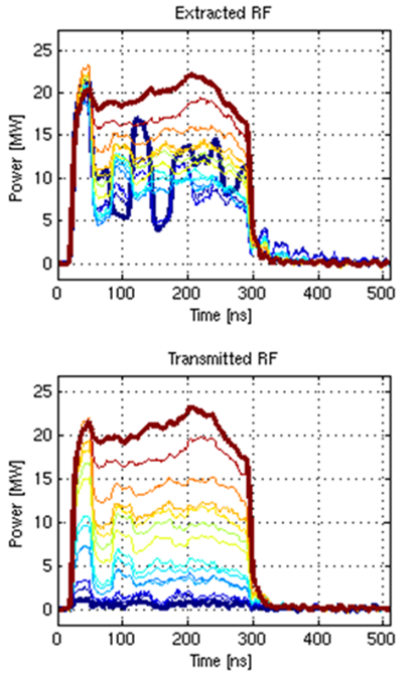

Figure 13: TBTS PETS ON/OFF demonstration with the beam. Here the line colors correspond to different settings of variable reflection. The colors are gradually changed from red (ON) to blue (OFF).

During experiments with the beam, the variable reflector settings were changed gradually from full reflection to full transmission. The RF powers produced by PETS and delivered to accelerating structure were measured at different intermediate piston positions. The results of one of the tests are shown in Fig. 13. These results were in a good agreement with the system computer modeling, where measured S-parameters of all components were used as an input [12].

At the time of the experiment, the available drive beam current in CTF3 made it impossible for us to run the system at the nominal CLIC RF power level in direct RF

power production mode. To demonstrate the power capability of the new RF components used in the ON/OFF RF circuit, we set the recirculation loop parameters to their amplification mode, similar to the setup that was routinely used in the TBTS PETS with external recirculation. The processing of the PETS with ON/OFF circuit went rather fast. In about 100 hours ($2x10^5$ pulses) the system was conditioned up to 150 MW × 200 ns. The PETS processing and operation history is summarized in Fig. 14 and Fig. 15.

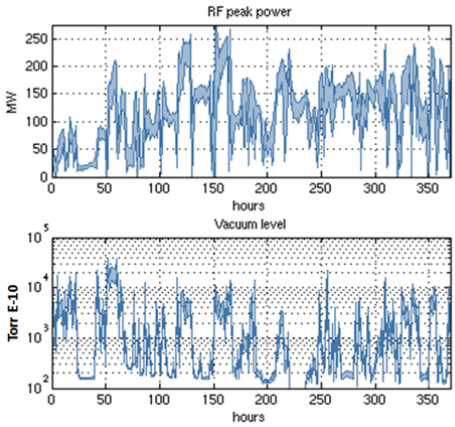

Figure 14: The PETS ON/OFF operation history: peak RF power (top) and vacuum level (bottom).

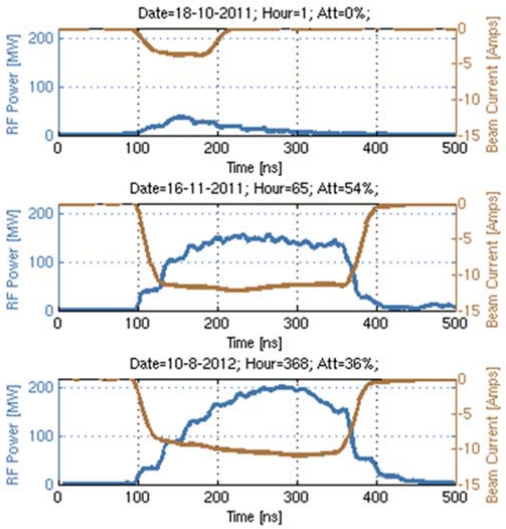

Figure 15: Typical drive beam current (brown lines) and RF power (blue lines) pulses at the different stages of operation.

2.7.2 **Summary**

The feasibility of all the issues associated with high RF power generation using the drive beam was successfully demonstrated in the dedicated testing program that was conducted at CERN during the period of 2008-2012.

The scaled, 1 m long, PETS was installed and operated in beam driven mode with external RF re-circulation in order to compensate for the lack of drive beam current and pulse length. The PETS routinely produced RF power with peak levels well in excess of the CLIC specifications.

The new high RF power variable RF reflector and variable RF short circuit were designed and fabricated. These devices have replaced the external recirculation in the special, 1 m long PETS installed in CTF3. The PETS ON/OFF operational principle and high peak RF power capability were successfully demonstrated in experiments with the CTF3 drive beam.

2.7.3 References

1. I. Syratchev *et al.,* 'High RF Power Production for CLIC', Proceedings of PAC 2007, Albuquerque, New Mexico, USA.
2. A. Candel *et al.,* "Numerical verification of the power transport and Wakefield coupling in the CLIC Two-Beam accelerator", SLAC-PUB-14439.
3. A. Cappelletti *et al.,* "Demonstration of the high RF power production feasibility in the CLIC power extraction and transfer structure [PETS]", NIMA, Vol. 667, Issue 1, pp. 78-81, 2011.
4. P. Skowronski *et al*., "The CLIC feasibility demonstration in CTF3", CERN-ATS-2011-117.
5. I. Syratchev *et al.,* 'CLIC RF High Power Production Testing Program', Proceedings of EPAC 2008, Genoa, Italy.
6. S. Kuzikov *et al.*, "A 12 GHz Pulse Compressor and Components for CLIC Test Stand", Proceedings of RuPAC-2010, Protvino, Russia.
7. R. Ruber and V. Ziemann, CERN CTF3 Note Report No. 092, 2009.
8. E. Adli, CERN CTF3 Note Report No. 096, 2009.
9. E. Adli *et al*., "*X*-band RF power production and deceleration in the two-beam test stand of the Compact Linear Collider test facility", PRST Accelerators and Beams, 14, 081001, 2011.
10. I. Syratchev, 'On-Off option and operation', 2nd CLIC Workshop 2008, Geneva, CERN.
11. I. Syratchev *et al*., "High Power Operation with Beam of a CLIC PETS Equipped with ON/OFF Mechanism", Proceedings of IPAC-2012, New Orleans, USA.
12. I. Syratchev, "The high power demonstration of the PETS ON/OFF operation", 5th High Gradient Workshop, KEK, Tsukuba, Japan, 2012.
13. Ansoft Corporation – HFSS: http://www.ansoft.com/

2.8 PACMAN (Particle Accelerator Components Metrology and Alignment to the Nanometer scale)

Nuria Catalán Lasheras, Helene Mainaud Durand, Michele Modena
CERN, CH 1211 Geneva 23, Switzerland
Mail to: helene.mainaud.durand@cern.ch

2.8.1 Introduction

The alignment of passive and active components along the CLIC accelerator shall reach unprecedented small values at micrometer level and with nanometer resolution. Indeed, this is a common requirement for the next generation of accelerators. Whether for producing a high number of collisions at the highest energy, or for producing the